

Effects of TiO₂ and Co₃O₄ Nanoparticles on Cell Cycle of a Pulmonary Cell Line (A549)

Silvana Pinelli¹, Diana Poli², Rossella Alinovi¹, Iris Banda¹, Giorgio Pelosi³, Marta Petyx⁴, Sergio Iavicoli⁴, Antonio Mutti¹, Paola Mozzoni¹, Matteo Goldoni^{1*}

¹Department of Medicine and Surgery, University of Parma, via Gramsci 14 43126 Parma, Italy

²Italian Workers' Compensation Authority (INAIL) Research Center at the University of Parma, via Gramsci 14 43126 Parma, Italy

³ Department of Chemistry, Life Sciences and Environmental Sustainability, University of Parma, Parco Area delle Scienze 17/A 43124 Parma, Italy

⁴Italian Workers' Compensation Authority (INAIL), Research Area, Department of Occupational Hygiene, via Fontana Candida, 1, 00040 Monte Porzio Catone Roma Italy

* Correspondence: Prof. Matteo Goldoni, matteo.goldoni@unipr.it; tel. +39 052 103 305 8

Silvana Pinelli: silvana.pinelli@unipr.it; Diana Poli: d.poli@inail.it; Rossella Alinovi: rossella.alinovi@unipr.it; Iris Banda: iris.banda@unipr.it; Giorgio Pelosi: giorgio.pelosi@unipr.it; Marta Petyx: m.petyx@inail.it; Sergio Iavicoli: s.iavicoli@inail.it; Antonio Mutti: antonio.mutti@unipr.it; Paola Mozzoni: paola.mozzoni@unipr.it; Matteo Goldoni: matteo.goldoni@unipr.it.

Abstract

The wide range of applications of nanoparticles (NPs) has increased the probability of environmental and occupational exposure. In a previous comparative study on cell line A549, we observed that oxidative stress caused by Co₃O₄ NPs affects the energetic homeostasis and the detoxification capacity, preventing autophagy induced by TiO₂ NPs. In this study, we have investigated the effects of NPs on the cell cycle.

Cytofluorimetric analysis showed a slow-down of the cell cycle progression for both NPs, with increases in the percentage of resting cells in the G0/G1. These observations were confirmed by a reduced expression of all cyclins, especially of CCNE1 and CDK2, involved in the late stages of the G1 phase, coupled with a significant increase in the expression of p21 only for Co₃O₄ NP exposure. On the contrary, the effects of TiO₂ NPs were modest. Cell cycle related miRNA-34a, miRNA-126 and miRNA-1290 resulted increased at different early time-points (4-8h) but were down-expressed at 24h-48h only after TiO₂ NP exposure. Our results show that NPs have an antiproliferative effect and deregulate cell cycle on A549 cells. These effects should not be underestimated because regulation of cycle progression is crucial for cell survival and repair of genetic damage.

Keywords: TiO₂, Co₃O₄, Nanoparticles, Cell Cycle, microRNA

1. Introduction

With an increasing number of commercial and consumer products containing nanoparticles (NPs), their use and production has become an important toxicological concern. The wide range of applications increases the possibility of human exposure (occupational and non-occupational), and therefore an improved understanding of their effects is required.

Among different NPs, Co_3O_4 NPs and TiO_2 NPs arose a great interest due to their wide range of applications, but also for their potential toxic properties [1]. Cobalt-based nanoparticles are used in many types of technological products: sensors, catalysts, pigments, and magnetism and energy storage devices leading to human occupational exposure.

Since inhalation is likely to be the main entry route of NPs into the human body, Co -NPs occupational exposure is commonly related to lung diseases, such as interstitial pneumonitis, fibrosis and asthma, and can increase the risk of developing lung cancer. In fact, lungs are the main potential exposure target organ during production and processing of nanomaterials that remain for a long time in the respiratory tract [2]. In addition, allergic dermatitis, and cardiomyopathy related to occupational exposure are also reported in the literature [3]. Since Co_3O_4 NPs are extensively used in biomedical applications such as orthopaedic prosthesis, internally non-occupational exposure can also occur [4]. This raises particular concerns about the potential risk of carcinogenicity [5].

TiO_2 NPs, on the other hand, are one of the earliest industrially produced and the most highly manufactured nanomaterials with a wide range of applications in various fields (e.g. paints, rubber, paper, cosmetics, pharmaceuticals and sunscreens). Over the last few years, the potential hazard of TiO_2 nanoparticles (NPs) has been debated and questioned [6].

The evolution of research on nanotoxicology demonstrates that not only apoptotic/necrotic experimental end-points or oxidative stress must be evaluated, but also that more emphasis should be addressed towards the sublethal and chronological mechanisms and pathways through which nanoparticles can impair cellular functions.

Insults from specific nanoparticulate formulations may abort the usual cell cycle and the phase arrest varies significantly depending on the NPs' composition, size, size distribution, surface, and coating [7]. Cell cycle progression should not be underestimated because it can be related to phenomena that lead cells to grow out of control, such as evasion of antigrowth signaling, abnormal proliferation and resistance to cell death, and other mechanisms involved in tumor formation and development of malignancy [8].

In addition, alterations of the normal cytokinesis mechanism may increase the possibility of nuclear re-fusion in cells that have finished nuclear division: nuclear fusion and cells with aneuploid chromosomes are frequently observed in tumors [9].

Several *in vitro* studies report similar abnormalities in cells exposed to cobalt nanoparticles, including DNA damage, micronucleus, induction and DNA strand breaks, mainly because of oxidative stress [1,10-13].

The potential toxicity of TiO₂ has been determined in different experimental investigations but it is still controversial. The potential hazardous effects of TiO₂ NPs on the cell cycle are still insufficient and the related mechanisms need further elucidation.

Several studies were carried out to understand if TiO₂ NPs induce cycle arrests and some of them excluded effects on cell cycle distribution [14]. However, perturbation of this process was reported in cells exposed to TiO₂ NPs [15-21].

These contradictory conclusions may be due to the varying experimental conditions, to the different cellular models and culture media, and to the different sizes of TiO₂ NPs. Moreover, synchronization was suggested to reveal alterations in cell cycle distribution that could be hidden in unsynchronized cell cultures [22]. Additionally, these discrepancies may also be ascribed to the metal NP interferences with fluorescent probes used in flow cytometric analysis of DNA [23].

Regulation of the cell cycle is crucial to cell survival, ensuring also the detection and repair of genetic damage as well as the prevention of uncontrolled cell division. Each phase occurs in a sequential irreversible fashion mediated by the two key classes of regulatory molecules, cyclins and cyclin-

dependent kinases (CDKs) [24,25]. While CDKs are constitutively expressed in cells, cyclins are synthesized at specific stages of the cell cycle in response to various molecular signals. Modification of the cell cycle checkpoint proteins, or of their expression, leads to abnormal progression. In this complex regulatory network, are involved also small noncoding RNA molecules, microRNAs (miRNAs) that inhibit the translation of mRNAs by binding to the 3'-untranslated region (UTR) of their target mRNAs, resulting in reduced levels of the corresponding protein or cleavage of their RNA [26]. We focused on three miRNA involved in the regulation of cycle: miRNA-34a, miRNA-126 and miRNA-1290 [27-29].

Therefore, we hypothesized that a thorough assessment of the factors controlling the cell cycle can contribute to the understanding of Co- and Ti-NP effects.

In our previous study, the cell cycle progression was significantly perturbed in human primary endothelial cell lines HAEC and HUVEC treated with Co_3O_4 NPs and TiO_2 NPs, with accumulation in phase G0/G1 [13]. The same NPs did not cause necrosis or apoptosis but significant decreases in the cell number and in the intracellular ATP levels in A549, a widely used cell line for pulmonary toxicity studies [1].

In this study, we have further investigated the effect of Co_3O_4 NPs and TiO_2 NPs on A549 cellular cycle and discussed their possible mechanisms, evaluating the expression of cyclins and of miRNAs as key post-transcriptional regulators of gene expression with effects on this process.

2. Results

2.1. Cellular cycle analysis

NPs effects on cell cycle progression were examined after 24, 48 and 72 hour exposure to 20 $\mu\text{g}/\text{ml}$ NPs. This concentration was chosen because in our previous study it did not cause cell death [1]. To avoid blunders arising from interference of probes with NPs, results generated by viability assays [1] were verified and confirmed by morphological observation and cell count (not shown).

The analysis of the cell cycle shows time-dependent perturbations for both NPs (Figure 1 and Table 1). Co_3O_4 NPs significantly altered cycle progression starting from 24 hours, causing accumulation of A549s in phase G0/G1 and decreases of S (24-48-72h) and G2/M (only at 72h) populations. This trend was also present during the treatment with TiO_2 NPs (Figure 1 and Table 1), but with some differences: (a) no significant effects were observed at 24h; (b) at 72h the percentage of cells in G0/G1 phase was lower than that observed for Co_3O_4 NPs; (c) the decrease of % of cells in S phase was lower than that observed for Co_3O_4 NPs.

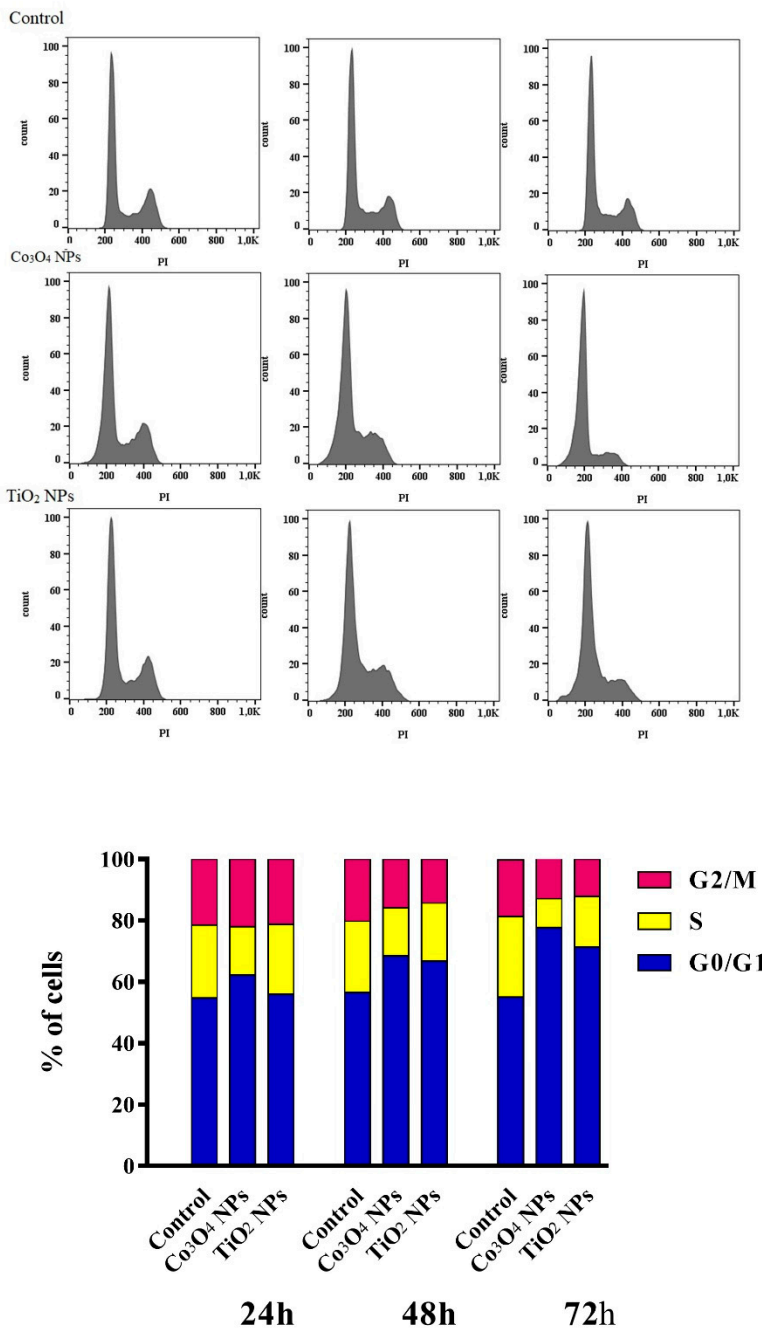


Figure 1. Monoparametric DNA analysis of the cellular cycle distribution after 24 h treatment with 20 $\mu\text{g}/\text{ml}$ NPs. Three distinct phases could be recognized in the proliferating cell population, corresponding to different peaks: G0/G1, S and G2/M phase.

Exposure	G0/G1 (%)	S (%)	G2/M (%)
Control 24h	54.8 (SD: 1.5)	23.7 (SD: 2.1)	21.5 (SD: 0.6)
Co ₃ O ₄ NPs 24h	62.2 (SD: 0.5) ^{*,**}	15.8 (SD: 0.4) ^{*,**}	22.0 (SD: 0.8)
TiO ₂ NPs 24h	56.0 (SD: 2.2)	22.7 (SD: 2.6)	21.3 (SD: 0.6)
Control 48h	56.7 (SD: 1.6)	23.2 (SD: 2.2)	20.2 (SD: 0.8)
Co ₃ O ₄ NPs 48h	68.5 (SD: 0.5) [*]	15.6 (SD: 0.7) [*]	15.9 (SD: 0.2)
TiO ₂ NPs 48h	66.7 (SD: 1.0) [*]	19.0 (SD: 2.6)	14.3 (SD: 3.5) [#]
Control 72h	55.1 (SD: 0.7)	26.3 (SD: 0.4)	18.6 (SD: 0.4)
Co ₃ O ₄ NPs 72h	77.7 (SD: 2.0) ^{*,**}	9.4 (SD: 1.4) ^{*,**}	12.9 (SD: 0.6) [*]
TiO ₂ NPs 72h	71.4 (SD: 1.3) [*]	16.5 (SD: 2.9) [*]	12.1 (SD: 1.6) [*]

Table 1: the percentage of cells in the three phases after 24-48-72h NP exposure. Means (SD) of three independent experiments are reported. [#]=p<0.05 vs control; ^{*}=p<0.01 vs control; ^{**}=p<0.01 vs TiO₂ NPs.

2.2. Cyclin expression

The alteration of the cell cycle was further assessed by the quantification of transcripts of cyclins and cyclin-dependent kinases involved in the control of the cycle in G0/G1 phase (Figure 2). This analysis was completed by the evaluation of p21 gene expression: p21 lead to the arrest of the cell cycle in G1, in response to different stressors stimuli. Co₃O₄ NPs caused a reduction of gene expression of all cyclins, although in different manner. The decrease was transient at 8 and/or 24 h for CDK4, CDK6 and CCNE1, with a total recovery after 48 hours from exposure, while a significant decrease at all the time-points was observed for CCND1 and CDK2. At the same time, a significant increase in the expression of p21 was observed only after 48h of treatment. During exposure to TiO₂ NPs, some cyclins involved in the early and late-phase G0/G1 were transiently hypo-expressed: CDK6 and CDK2 at 8 hours and CCNE1 at 24 hours from exposure, with a total recovery after 48 hours. p21 gene was not upregulated.

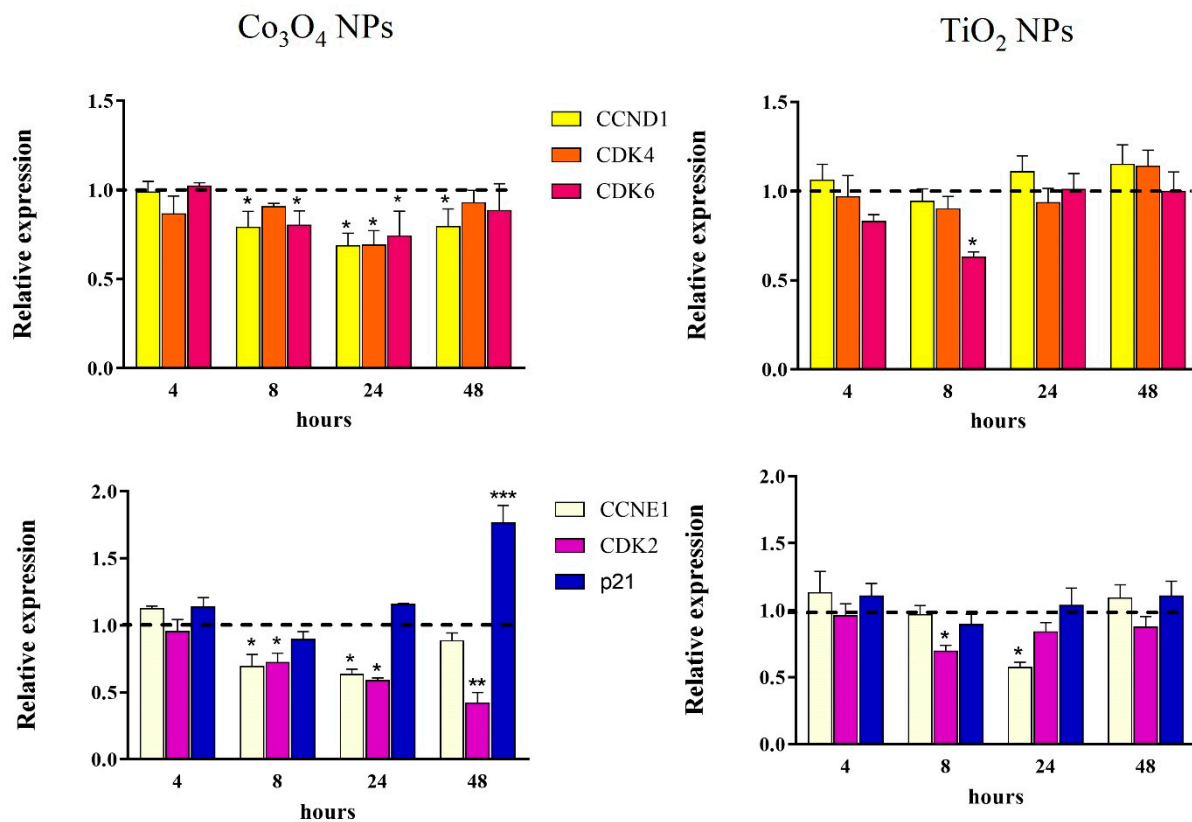


Figure 2. Relative changes in cyclin expression, cyclin-dependent kinases (CDKs) and p21 (vs untreated controls) in human A549 cells during NPs exposure. Significantly different from control: *: $p < 0.05$; **: $p < 0.01$; ***: $p < 0.001$.

2.3. MiRNA expression

We also evaluated the expression of three miRNAs involved in the regulation of the cell cycle (Figure 3). The expression of all miRNA varied over time in response to the presence of NPs. MiRNAs 34a and 126 were induced two- to fourfold in the early stages of exposure and then their levels fell to values lower than the controls. The pattern at early times was similar for both nanoparticles, although miRNA-34a increase seems to be more important for Co₃O₄ NPs and miRNA-126 for TiO₂ NPs. However, after exposure at later time TiO₂ NPs reduced the expression of both, while with Co₃O₄ NPs a modest under-expression was observed at 48 hours only for miRNA-126.

More complex was the trend of miRNA-1290: a slight upregulation in the early hours of Co_3O_4 NPs exposure was followed by a transient decrease and then by an overexpression from 24h until the end of the observation period. This biphasic trend was also observed in cells exposed to TiO_2 NPs though at lower levels.

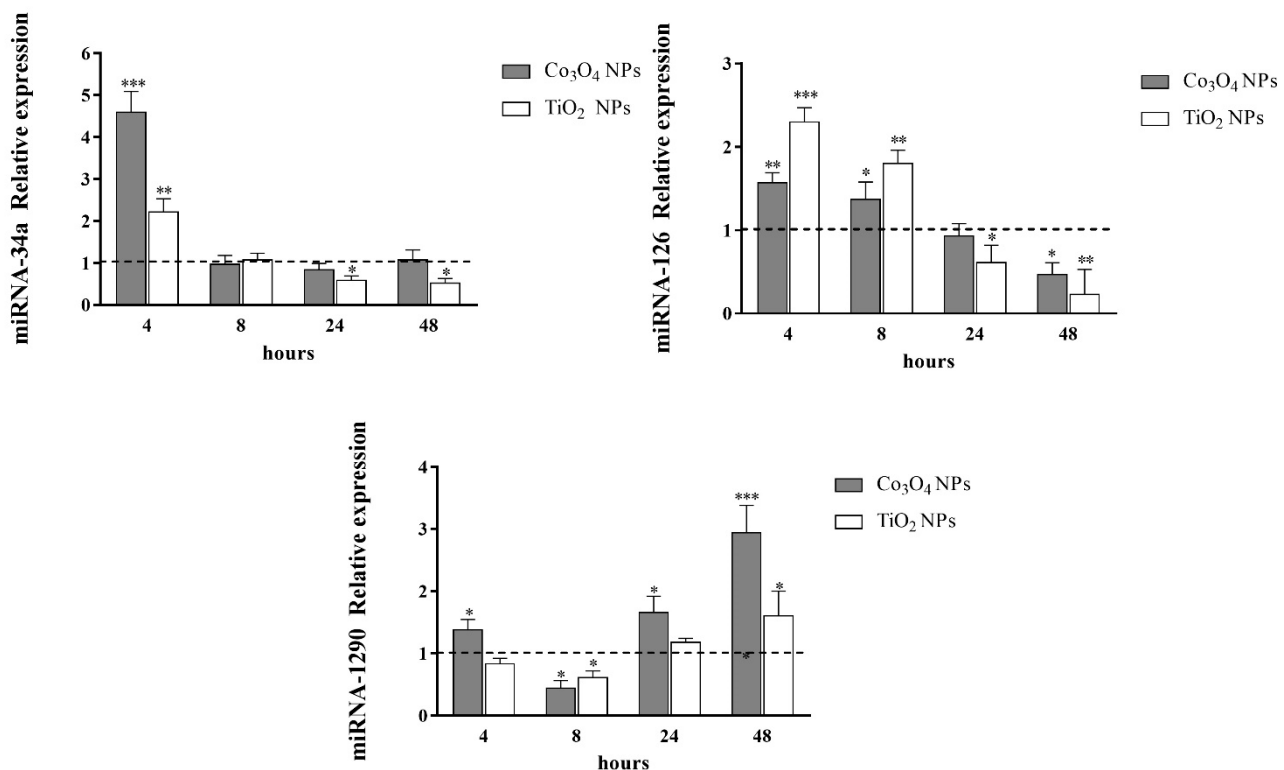


Figure 3. Relative expression changes of miRNA-34a, miRNA-126 and miRNA-1290 (*vs* untreated controls) in human A549 cells during NPs exposure. Significantly different from control: *: $p < 0.05$; **: $p < 0.01$; ***: $p < 0.001$.

3. Discussion

Although a widespread opinion attributes the effects of metallic NPs mainly to oxidative stress, NPs can induce cellular responses via different pathways, not involving the redox imbalance. We confirmed this in our previous studies [1] comparing nano-sized Co oxide to Ti oxide for a long time considered “safe” non-toxic and frequently used as a negative control when assessing nanotoxicity. Both NPs caused neither necrosis nor apoptosis, but the persistent presence of both NPs resulted in a significant decrease of cell number and of clonogenic activity.

Oxidative stress was evident only for Co_3O_4 NPs, influencing energy homeostasis and hampering the ability to detoxify and to repair the resulting damage, thus preventing the induction of autophagy. Instead, TiO_2 NPs elicit autophagy also under sub-toxic conditions [1].

Cytofluorimetric analysis showed a slow-down of the cell cycle progression for both NPs, with increases in the percentage of resting cells in the G0/G1, more pronounced after 48 hour exposure for Co_3O_4 NPs.

Antiproliferative effects of these NPs, but particularly of Co_3O_4 NPs, were observed also in endothelial primary cells [13], coupled with perturbations of the cell cycle and accumulation of HAECs and HUVECs in phase G0/G1. Our present work has confirmed this effect also in the quickly dividing human lung cancer cells A549: both included NPs are able to slowing down the cycle progression, but Co_3O_4 NPs were more active.

If disturbances of Co_3O_4 NPs on the cell cycle are frequently reported and accepted [13], the evidence for the TiO_2 NPs is more controversial and even the phase in which a block occurs is undefined/debated. In other *in vitro* and *in vivo* systems, changes in cell cycle progression were observed in the short- and long-term [30,31] and these disturbances seem to affect mitotic progression at anaphase and telophase leading to chromosomal instability and cell transformation. Other authors suggested that TiO_2 NPs could interfere with DNA synthesis and lead to a delay in cell cycle progression in the S phase [16,32]. In A549 cells a G2/M phase arrest was induced by TiO_2 NPs [17,18]. Recently, it has been observed different responses to TiO_2 NPs in model cell lines

constitutive of the alveolo-capillary barrier, and that, in A549, the cell cycle progression was not impacted by TiO₂ NPs exposure [20]. Furthermore, TiO₂ NP-exposed cells without synchronization had no changes in cell cycle distribution; however, synchronized cells also reveal a faster capability of TiO₂ NP-exposed cells to increase cell population in the G2/M phase, concluding that synchronization discloses a greater percentage of cells in the G2/M phase and higher proliferation than TiO₂ NP-synchronized cells [22].

Regulation of the cell cycle involves processes crucial to cell survival, including the detection and repair of genetic damage to ensure that damaged or incomplete DNA is not passed on to daughter cells. The prevention of gaps in replication is very important, because ensures that every portion of the cell genome will be replicated once and only once: daughter cells that are missing all or part of crucial genes will die. Two key classes of regulatory molecules determine the cell's progress into the cycle: cyclins and cyclin-dependent kinases (CDKs) [24,25]. The close interaction of CDKs with cyclins and Cdk inhibitors (CKIs) is necessary for ensuring orderly progression through the cell cycle. These molecules act in concert in a cascade.

Cyclin D is the first cyclin produced in response to extracellular signals and binds to existing CDK4, forming the active cyclin D-CDK4 complex. This complex, in turn, phosphorylates the retinoblastoma susceptibility protein (Rb), causing the dissociation of E2F/DP1/Rb complex and activating E2F. This activation triggers the transcription of various genes such as cyclin E, cyclin A, DNA polymerase, and thymidine kinase. Cyclin E, then, binds to CDK2 and the cyclin E-CDK2 complex drives the cell from the G1 to the S phase (G1/S transition). The complex cyclin B-CDK1 initiates the G2/M phase: its activation causes the breakdown of the nuclear membrane and the initiation of prophase, while subsequently, its deactivation causes the cell to exit mitosis. Two main checkpoints are present: the G1/S checkpoint, a rate limiting step, and the G2/M checkpoint. Cell cycle checkpoints are control mechanisms that ensure the fidelity of cell division, verifying whether the processes at each phase of the cell cycle have been accurately completed before progression into the next phase. All checkpoints allows to monitor and regulate the progression at specific points and

ensures that the cell is prepared for the following steps: the next phase cannot be started until checkpoint requirements have been verify. It is impossible to “reverse” the cycle.

In this work we observed a decreased expression of cyclins and CDk involved in the regulation of the early and late stage of phase G0/G1 and these results are consistent with the accumulation of resting cells evidenced in cytofluorimetric analysis. The differences in antiproliferative activity between Co and TiO₂ NPs were furthermore confirmed by the lower downregulation of Cyclin and CDKs during TiO₂ NPs exposure of A549. After TiO₂ NP exposure, only three cyclins were under-expressed at single time-points, while after Co₃O₄ NP exposure the decrease was transient for CDK4, CDK6 and CCNE1, and permanent for CCND1 and CDK2. To this different response may also contribute p21, the potent cyclin-dependent kinase inhibitor (CKI): the p21 (CIP1/WAF1) protein binds to and inhibits the activity of cyclin-CDK2, -CDK1, and -CDK4/6 complexes, and thus functions as a regulator of the cell cycle progression at G₁ and S phase [33,34]. Only after Co₃O₄ NP treatment, the levels of p21 were elevated and rose to their highest levels at the end of the observation period.

Results therefore indicate that cyclin expression alone cannot fully justify the arrest of cell cycle in G0/G1 phase after TiO₂ NP exposure. Therefore, we speculate that autophagy observed in our previous work [1] may play a role. Although the relationship between autophagy and G0/G1 phase arrest in the absence of cellular death is poorly documented in literature with NPs, this has been demonstrated for some drugs, like metformin [35].

More difficult is the interpretation of miRNA expression in A549 cells during NP exposure. Loss of miRNA-34a expression or inactivation has been identified in many tumor types (lung, breast, colon, kidney, bladder, pancreatic cancer and melanoma) and in cell lines derived from the corresponding tumors. miRNA-34a is directly controlled by tumor protein p53 at the transcriptional level and conversely miRNA-34a can stimulate endogenous p53 activity in a positive feedback [36,37]. In response to p53 activation, miRNA-34a up-regulation significantly decreased CDK4 and E2F1 protein levels, leading to G0/G1 cell cycle arrest [38]. An ectopic expression of miR-34a leads to a dramatic reprogramming of target genes and consequently inhibits cancer cell proliferation, induces

cell cycle arrest, and may enhance apoptosis [36,37,39-41]. Its anticancer activity has been demonstrated in various human cancer cells *in vitro* and is considered one of the most promising tumor suppressive miRNAs for cancer treatment [42].

Among various miRNAs, miRNA-126 has an important role in cancer progression via negative control of proliferation, migration, invasion and cell survival, suppressing translation of different target genes [43]. Anti-proliferative effect of miRNA-126 was found in several tumor types including colon cancer, non-small cell lung cancer and malignant mesothelioma (MM) [44-46].

MiRNA-1290 is encoded in the first intron of the ALDH4A1 gene in the human genome, and its expression has only been described in humans. Homologs are present in primates but not in other vertebrates, while the mature miRNA-1290 sequence is exclusive to the subfamily Homininae [29]. miRNA-1290 can play a role in mitotic exit during differentiation by regulating the expression of key cell cycle proteins and in maintaining cell cycle repression and differentiated state [29]. Its targets include genes coding for proteins involved in cell cycle arrest, G1/S transition and interphase, such as cyclins, cyclin kinases and cyclin kinase inhibitors. miRNA-1290 overexpression led to a slowing down of the cell cycle and differentiation [29,47,48].

The expression of these three miRNA was transiently increased during treatment with both NPs, but at different times-points. MiRNA-34a and miRNA-126 are more involved/active in the early phase while miRNA-1290 supports the last cellular exposure. However, a late under-expression of miRNA-34a and miRNA-126 was observed after TiO₂ exposure, in line with a similar phenomenon observed for miRNA associated with autophagy [1]. These observations complicate the interpretation of their roles but is inherent to the intrinsic nature of these molecules to be very versatile and easily influenced by feedback mechanisms. MiRNAs can regulate the target gene by imperfect base-pairing to the 3' UTR, so a single miRNA can target several hundred mRNAs. Moreover, a single target gene often includes more binding sites for multiple miRNAs that can bind co-operatively [49,50], allowing miRNAs to form a complex regulatory control network. The high time-dependent variation in intracellular levels of miRNA is an additional confounding factor in the interpretation of their role.

Conclusions

Our results provide a clear demonstration that NPs have an antiproliferative effect on A549 cells and deregulate cell cycle progression, although the mechanisms seem partially different for CO_3O_4 and TiO_2 NPs. Further studies are necessary to understand the molecular mechanism under the relationship between autophagy, G0/G1 phase arrest and under-expression of several miRNAs at 24-48 hours after TiO_2 NPs exposure. However, these effects should not be underestimated, because regulation of the cycle progression is crucial for cell survival, ensuring the detection and repair of genetic damage, and prevents cells from escaping the control mechanisms essential for the maintenance of tissue homeostasis. In long-term exposed cells, this may have very serious consequences, because errors in these processes can either kill a cell, for example through apoptosis, or cause mutations that may lead to cancer.

4. Materials and Methods

4.1. Nanoparticle Characterization

Cobalt (II,III) oxide nanopowder (<50 nm) and TiO₂ nanopowder (<100 nm) are commercially available and were provided with physicochemical characterization by Sigma (St. Louis, MO, USA). In Alinovi *et al.* 2015, the complete characterization of NPs is reported [13]. The CoNPs and the TiO₂ NPs were investigated by Transmission Electron Microscopy (TEM) once they were dispersed in complete medium to visualize the dimensions of the NPs and the aggregation state. In addition, by performing electron diffraction experiments, the crystalline phases of the nanopowder were checked. The dominant phase observed for the NPs is anatase (>90%), while a small amount of the NPs show a rutile structure. Since the behavior and the aggregation state of the NPs in different mediums depend strongly on the surface charge of the NPs and the ionic strength of the suspension, a further characterization using both Dynamic Light Scattering and Z-potential techniques was carried out. The analysis was performed using the 90Plus PALS instrument (Brookhaven Corp., Holtsville, NY, USA).

4.2. Cell culture and treatment

The human non-small cell lung cancer A549 cell line was obtained by ATCC. Cells were routinely cultured in sterile plastic material from Costar, Corning (Amsterdam, The Netherlands) and in RPMI 1640 medium (Euroclone, Milan, Italy) supplemented with 10% fetal bovine serum and penicillin/streptomycin (100 U/ml+0.1 mg/ml) and maintained in a humidified atmosphere with 5% CO₂ at 37°C. The cells were incubated for 24h prior to exposure to NPs. Cells free of NPs served as the control group in each assay.

To distribute the nanoparticles in the working solution as evenly as possible, before each cell culture experiment, their suspensions were sonicated immediately before use [13].

The morphology of the cells was evaluated using an inverted microscope (Olympus CK40-RFL, Tokyo, Japan).

4.3. Cell cycle analysis

The quantification of DNA content by flow cytometry is the most used method for the identification of the cell distribution during the phases of the cell cycle. Nuclear DNA content was labelled with propidium iodide (PI) as previously described [51]. Briefly, about 1×10^6 cells were harvested, resuspended in PBS (Ca^{2+} and Mg^{2+} free and supplemented with EDTA 0.5 mM) and fixed adding 96% cold ethanol. After overnight incubation at 4°C , samples were washed and incubated with 1 ml of PBS containing 20 $\mu\text{g}/\text{ml}$ PI and 12.5 μL RNase (1 mg/ml in water), then stained cells were sorted by a FC500TM flow cytometer (Instrumentation Laboratory, Bedford, MA, USA). At least 20,000 events were counted. The percentages of cells occupying the different phases of the cell cycle were calculated by FlowJo Software (Tree Star Inc, Ashland, OR, U.S.A.).

4.4 RNA Isolation and cDNA Synthesis

RNA isolated from cultured cells using TRIzol reagent (Thermo Fisher Scientific, MA USA) was quantified using a NanoDrop spectrophotometer (Thermo Scientific, DE), after removing any genomic DNA contamination [1].

The gene expression of CDK4, CCND1, CDK6, CCNE1, CDK2 and p21 was assessed using real-time quantitative reverse transcription-polymerase chain reaction (qRT-PCR) on an iCycler iQ Multicolor RealTime PCR Detection System (Bio-Rad, Hercules, CA, USA). Specific primers (spanning the exon-exon junctions) and locked nucleic acid probes (Table 2) were designed using ProbeFinder software (Roche Diagnostics, Mannheim, Germany), and the related transcript was quantified using the *geNorm* algorithm for Microsoft ExcelTM after normalization by the expression

of the control genes (phosphoglycerate kinase 1 [*PGK1*], ribosomal protein L13 [*RPL13*], hypoxanthine-guanine phosphoribosyltransferase [*HPRT*]), and expressed as arbitrary units.

Table 2: Primers and probes used for gene expression.

GENE	PRIMER FORWARD	PRIMER REVERSE	PROBE
CDK2	5' AAAGCCAGAAACAAGTTGACG 3'	5' GTACTGGGCACACCCTCAGT 3'	5' FAM GGTGGTGG 3' DQ
CDK4	5' GTGCAGTCGGTGGTACCTG 3'	5' TTGCGTTGTGTGGGTTAAAA 3'	5' FAM TGGAGGAG 3' DQ
CDK6	5' TGATCAACTAGGAAAAATCTTGG 3'	5' GGCAACATCTCTTAGGCCAGT 3'	5' FAM CAGGAGAA 3' DQ
CCND1	5' GCTGTGCATCTACACCGACA 3'	5' TTGAGCTTGTTCACCAGGAG 3'	5' FAM AGGAGCTG 3' DQ
CCNE1	5' GGCCAAAATCGACAGGAC 3'	5' GGGTCTGCACAGACTGCAT 3'	5' FAM GGAGCCAG 3' DQ
P21	5' TCACTGTCTTGACCCTTGTGC 3'	5' GGCGTTGGAGTGGTAGAAA 3'	5' FAM CCTGGAGA 3' DQ
RPL13	5'GGAGAACCTCCGCTTCAT3'	5'CTGGCTCGGCTTAACCTT3'	5' FAM GGAGGAAG 3' DQ
HPRT	5'TGACCTTGATTTATTTGCATACC3'	5'CGAGCAAGACGTTCAGTCCT3'	5' FAM GCTGAGGA 3' DQ
RPL13	5'ACAGCTGCTCAGCTTCACCT3'	5'TGGCAGCATGCCATAAATAG3'	5' FAM CAGTGGCA 3' DQ

4.5. Reverse transcription and quantification of miRNA expression by qRT-PCR

Total RNA was reverse transcribed using a TaqMan MicroRNA RT kit (Thermo Fisher Scientific, MA USA), as previously described [1]. cDNA was amplified using TaqMan 2x Universal PCR Master Mix (Life Technologies, Carlsbad, CA), a specific primer set, and hydrolysis probe-based TaqMan microRNA Assays (Life Technologies, Carlsbad, CA) in 20 μ L of mixture. Quantitative PCR was performed using an iCycler iQ RealTime Detection System (Bio-Rad, Hercules, CA). The reactions consisted of one step at 95°C for 10 min, followed by 40 cycles of 95°C for 15 s and 60°C for 1 min. All assays were made in duplicate, and one no-template and two interpolate controls were used in each experiment. The expression of the miRNAs was calculated using the comparative cycle threshold (Ct) method, as the fractional cycle number at which the fluorescence passed the fixed threshold. The Ct values of the target miRNAs were normalized to sno-RNU6B and the fold-change in expression of each miRNA were calculated using the equation $2^{-\Delta\Delta Ct}$ [52].

4.6. Statistical analysis

SPSS software version 20.0 (SPSS Inc/IBM, Chicago, Ill, USA) was used for analysis. Data of almost three independent experiments are presented as mean \pm standard deviation and all groups were analyzed using two-way ANOVA followed by Dunnett's or Tukey's post-hoc test. Statistical significance was set at $p<0.05$ (two-sided).

Acknowledgements

This study was supported by the Ministry of Health, Italy Ricerca Finalizzata 2009 Grant: Integrated approach to evaluating the biological effects on lung, cardiovascular system and skin of occupational exposure to nanomaterials (NanO I-LuCaS). RF-2009-1472550.

Conflicts of Interest

The authors declare no conflict of interest.

Authors' Contribution

"Conceptualization, S.P., R.A., P.M.; Methodology, S.P., R.A., P.M., M.G.; Formal Analysis, G.P.; Data Curation, M.G.; Writing – Original Draft Preparation, S.P., D.P., R.A., P.M., M.G.; Writing – Review & Editing, G.P., I.B., M.P, S.I., A.M; Supervision, A.M., M.G.; Project Administration, S.I.; Funding Acquisition, S.I., A.M."

References

1. Alinovi, R.; Goldoni, M.; Pinelli, S.; Ravanetti, F.; Galetti, M.; Pelosi, G.; De Palma, G.; Apostoli, P.; Cacchioli, A.; Mutti, A., *et al.* Titanium dioxide aggregating nanoparticles induce autophagy and under-expression of microRNA 21 and 30a in a549 cell line: A comparative study with cobalt(ii, iii) oxide nanoparticles. *Toxicol. In Vitro* **2017**, *42*, 76-85.
2. Kendall, M.; Holgate, S. Health impact and toxicological effects of nanomaterials in the lung. *Respirology* **2012**, *17*, 743-758.
3. Klasson, M.; Bryngelsson, I.L.; Pettersson, C.; Husby, B.; Arvidsson, H.; Westberg, H. Occupational exposure to cobalt and tungsten in the swedish hard metal industry: Air concentrations of particle mass, number, and surface area. *Ann. Occup. Hyg.* **2016**, *60*, 684-699.
4. Ladon, D.; Doherty, A.; Newson, R.; Turner, J.; Bhamra, M.; Case, C.P. Changes in metal levels and chromosome aberrations in the peripheral blood of patients after metal-on-metal hip arthroplasty. *J. Arthroplasty* **2004**, *19*, 78-83.
5. MHRA. *Medical device alert: All metal-on-metal (mom) hip replacements (ref: Mda/2010/033)*. Medicines and Healthcare products Regulatory Agency: London, UK, 2010.
6. Iavicoli, I.; Leso, V.; Fontana, L.; Bergamaschi, A. Toxicological effects of titanium dioxide nanoparticles: A review of in vitro mammalian studies. *Eur. Rev. Med. Pharmacol. Sci.* **2011**, *15*, 481-508.
7. Huang, Y.W.; Cambre, M.; Lee, H.J. The toxicity of nanoparticles depends on multiple molecular and physicochemical mechanisms. *Intl. J. Mol. Sci.* **2017**, *18*.
8. Wiman, K.G.; Zhivotovsky, B. Understanding cell cycle and cell death regulation provides novel weapons against human diseases. *J. Intern. Med.* **2017**, *281*, 483-495.
9. Lacroix, B.; Maddox, A.S. Cytokinesis, ploidy and aneuploidy. *J. Pathol.* **2012**, *226*, 338-351.
10. Alarifi, S.; Ali, D.; Y, A.O.; Ahamed, M.; Siddiqui, M.A.; Al-Khedhairy, A.A. Oxidative stress contributes to cobalt oxide nanoparticles-induced cytotoxicity and DNA damage in human hepatocarcinoma cells. *Intl. J. Nanomed.* **2013**, *8*, 189-199.
11. Wan, R.; Mo, Y.; Feng, L.; Chien, S.; Tollerud, D.J.; Zhang, Q. DNA damage caused by metal nanoparticles: Involvement of oxidative stress and activation of atm. *Chem. Res. Toxicol.* **2012**, *25*, 1402-1411.
12. Cavallo, D.; Ciervo, A.; Fresegnna, A.M.; Maiello, R.; Tassone, P.; Buresti, G.; Casciardi, S.; Iavicoli, S.; Ursini, C.L. Investigation on cobalt-oxide nanoparticles cyto-genotoxicity and inflammatory response in two types of respiratory cells. *J. Appl. Toxicol.* **2015**, *35*, 1102-1113.
13. Alinovi, R.; Goldoni, M.; Pinelli, S.; Campanini, M.; Aliatis, I.; Bersani, D.; Lottici, P.P.; Iavicoli, S.; Petyx, M.; Mozzoni, P., *et al.* Oxidative and pro-inflammatory effects of cobalt and titanium oxide nanoparticles on aortic and venous endothelial cells. *Toxicol. In Vitro* **2015**, *29*, 426-437.
14. Tucci, P.; Porta, G.; Agostini, M.; Dinsdale, D.; Iavicoli, I.; Cain, K.; Finazzi-Agro, A.; Melino, G.; Willis, A. Metabolic effects of tio2 nanoparticles, a common component of sunscreens and cosmetics, on human keratinocytes. *Cell Death Dis.* **2013**, *4*, e549.
15. Hou, Y.; Cai, K.; Li, J.; Chen, X.; Lai, M.; Hu, Y.; Luo, Z.; Ding, X.; Xu, D. Effects of titanium nanoparticles on adhesion, migration, proliferation, and differentiation of mesenchymal stem cells. *Intl. J. Nanomed.* **2013**, *8*, 3619-3630.
16. Prasad, R.Y.; Wallace, K.; Daniel, K.M.; Tennant, A.H.; Zucker, R.M.; Strickland, J.; Dreher, K.; Kligerman, A.D.; Blackman, C.F.; Demarini, D.M. Effect of treatment media on the agglomeration of titanium dioxide nanoparticles: Impact on genotoxicity, cellular interaction, and cell cycle. *ACS Nano* **2013**, *7*, 1929-1942.

17. Wang, Y.; Cui, H.; Zhou, J.; Li, F.; Wang, J.; Chen, M.; Liu, Q. Cytotoxicity, DNA damage, and apoptosis induced by titanium dioxide nanoparticles in human non-small cell lung cancer a549 cells. *Environ. Sci. Pollut. Res. Intl.* **2015**, *22*, 5519-5530.
18. Kansara, K.; Patel, P.; Shah, D.; Shukla, R.K.; Singh, S.; Kumar, A.; Dhawan, A. Tio2 nanoparticles induce DNA double strand breaks and cell cycle arrest in human alveolar cells. *Environ. Mol. Mutagen.* **2015**, *56*, 204-217.
19. Periasamy, V.S.; Athinarayanan, J.; Al-Hadi, A.M.; Juhaimi, F.A.; Alshatwi, A.A. Effects of titanium dioxide nanoparticles isolated from confectionery products on the metabolic stress pathway in human lung fibroblast cells. *Arch. Environ. Contam. Toxicol.* **2015**, *68*, 521-533.
20. Hanot-Roy, M.; Tubeuf, E.; Guilbert, A.; Bado-Nilles, A.; Vigneron, P.; Trouiller, B.; Braun, A.; Lacroix, G. Oxidative stress pathways involved in cytotoxicity and genotoxicity of titanium dioxide (tio2) nanoparticles on cells constitutive of alveolo-capillary barrier in vitro. *Toxicol. In Vitro* **2016**, *33*, 125-135.
21. Armand, L.; Biola-Clier, M.; Bobyk, L.; Collin-Faure, V.; Diemer, H.; Strub, J.M.; Cianferani, S.; Van Dorsselaer, A.; Herlin-Boime, N.; Rabilloud, T., *et al.* Molecular responses of alveolar epithelial a549 cells to chronic exposure to titanium dioxide nanoparticles: A proteomic view. *J. Proteomics* **2016**, *134*, 163-173.
22. Medina-Reyes, E.I.; Bucio-Lopez, L.; Freyre-Fonseca, V.; Sanchez-Perez, Y.; Garcia-Cuellar, C.M.; Morales-Barcenas, R.; Pedraza-Chaverri, J.; Chirino, Y.I. Cell cycle synchronization reveals greater g2/m-phase accumulation of lung epithelial cells exposed to titanium dioxide nanoparticles. *Environ. Sci. Pollut. Res. Intl.* **2015**, *22*, 3976-3982.
23. Darolles, C.; Sage, N.; Armengaud, J.; Malard, V. In vitro assessment of cobalt oxide particle toxicity: Identifying and circumventing interference. *Toxicol. In Vitro* **2013**, *27*, 1699-1710.
24. Mahmoudi, M.; Azadmanesh, K.; Shokrgozar, M.A.; Journeay, W.S.; Laurent, S. Effect of nanoparticles on the cell life cycle. *Chem. Rev.* **2011**, *111*, 3407-3432.
25. Lim, S.; Kaldis, P. Cdks, cyclins and ckis: Roles beyond cell cycle regulation. *Development* **2013**, *140*, 3079-3093.
26. Otsuka, K.; Ochiya, T. Genetic networks lead and follow tumor development: Microrna regulation of cell cycle and apoptosis in the p53 pathways. *Biomed. Res. Intl.* **2014**, *2014*, 749724.
27. Chen, F.; Hu, S.J. Effect of microrna-34a in cell cycle, differentiation, and apoptosis: A review. *J. Biochem. Mol. Toxicol.* **2012**, *26*, 79-86.
28. Luo, J.; Zhu, C.; Wang, H.; Yu, L.; Zhou, J. Microrna-126 affects ovarian cancer cell differentiation and invasion by modulating expression of vascular endothelial growth factor. *Oncol. Lett.* **2018**, *15*, 5803-5808.
29. Yelamanchili, S.V.; Morsey, B.; Harrison, E.B.; Rennard, D.A.; Emanuel, K.; Thapa, I.; Bastola, D.R.; Fox, H.S. The evolutionary young mir-1290 favors mitotic exit and differentiation of human neural progenitors through altering the cell cycle proteins. *Cell Death Dis.* **2014**, *5*, e982.
30. Wu, J.; Sun, J.; Xue, Y. Involvement of jnk and p53 activation in g2/m cell cycle arrest and apoptosis induced by titanium dioxide nanoparticles in neuron cells. *Toxicol. Lett.* **2010**, *199*, 269-276.
31. Huang, S.; Chueh, P.J.; Lin, Y.W.; Shih, T.S.; Chuang, S.M. Disturbed mitotic progression and genome segregation are involved in cell transformation mediated by nano-tio2 long-term exposure. *Toxicol. Appl. Pharmacol.* **2009**, *241*, 182-194.
32. Gao, X.; Wang, Y.; Peng, S.; Yue, B.; Fan, C.; Chen, W.; Li, X. Comparative toxicities of bismuth oxybromide and titanium dioxide exposure on human skin keratinocyte cells. *Chemosphere* **2015**, *135*, 83-93.
33. Karimian, A.; Ahmadi, Y.; Yousefi, B. Multiple functions of p21 in cell cycle, apoptosis and transcriptional regulation after DNA damage. *DNA Repair* **2016**, *42*, 63-71.

34. Georgakilas, A.G.; Martin, O.A.; Bonner, W.M. P21: A two-faced genome guardian. *Trends Mol. Med.* **2017**, *23*, 310-319.

35. Wang, Y.; Xu, W.; Yan, Z.; Zhao, W.; Mi, J.; Li, J.; Yan, H. Metformin induces autophagy and g0/g1 phase cell cycle arrest in myeloma by targeting the ampk/mtorc1 and mtorc2 pathways. *J. Exp. Clin. Cancer Res.* **2018**, *37*, 63.

36. He, L.; He, X.; Lim, L.P.; de Stanchina, E.; Xuan, Z.; Liang, Y.; Xue, W.; Zender, L.; Magnus, J.; Ridzon, D., *et al.* A microrna component of the p53 tumour suppressor network. *Nature* **2007**, *447*, 1130-1134.

37. Yamakuchi, M.; Ferlito, M.; Lowenstein, C.J. Mir-34a repression of sirt1 regulates apoptosis. *Proc. Natl. Acad. Sci. USA* **2008**, *105*, 13421-13426.

38. Lin, J.; Jin, X.; Bu, Y.; Cao, D.; Zhang, N.; Li, S.; Sun, Q.; Tan, C.; Gao, C.; Jiang, Y. Efficient synthesis of rita and its analogues: Derivation of analogues with improved antiproliferative activity via modulation of p53/mir-34a pathway. *Org. Biomol. Chem.* **2012**, *10*, 9734-9746.

39. Kasinski, A.L.; Slack, F.J. Mirna-34 prevents cancer initiation and progression in a therapeutically resistant k-ras and p53-induced mouse model of lung adenocarcinoma. *Cancer Res.* **2012**, *72*, 5576-5587.

40. Liu, K.; Huang, J.; Xie, M.; Yu, Y.; Zhu, S.; Kang, R.; Cao, L.; Tang, D.; Duan, X. Mir34a regulates autophagy and apoptosis by targeting hmgb1 in the retinoblastoma cell. *Autophagy* **2014**, *10*, 442-452.

41. Ma, Z.L.; Hou, P.P.; Li, Y.L.; Wang, D.T.; Yuan, T.W.; Wei, J.L.; Zhao, B.T.; Lou, J.T.; Zhao, X.T.; Jin, Y., *et al.* Microrna-34a inhibits the proliferation and promotes the apoptosis of non-small cell lung cancer h1299 cell line by targeting tgfβtar2. *Tumour Biol.* **2015**, *36*, 2481-2490.

42. Wang, W.P.; Ho, P.Y.; Chen, Q.X.; Addepalli, B.; Limbach, P.A.; Li, M.M.; Wu, W.J.; Jilek, J.L.; Qiu, J.X.; Zhang, H.J., *et al.* Bioengineering novel chimeric microrna-34a for prodrug cancer therapy: High-yield expression and purification, and structural and functional characterization. *J. Pharmacol. Exp. Ther.* **2015**, *354*, 131-141.

43. Ebrahimi, F.; Gopalan, V.; Smith, R.A.; Lam, A.K. Mir-126 in human cancers: Clinical roles and current perspectives. *Exp. Mol. Pathol.* **2014**, *96*, 98-107.

44. Guo, C.; Sah, J.F.; Beard, L.; Willson, J.K.; Markowitz, S.D.; Guda, K. The noncoding rna, mir-126, suppresses the growth of neoplastic cells by targeting phosphatidylinositol 3-kinase signaling and is frequently lost in colon cancers. *Genes Chromosomes Cancer* **2008**, *47*, 939-946.

45. Chen, S.W.; Wang, T.B.; Tian, Y.H.; Zheng, Y.G. Down-regulation of microrna-126 and microrna-133b acts as novel predictor biomarkers in progression and metastasis of non small cell lung cancer. *Intl. J. Clin. Exp. Pathol.* **2015**, *8*, 14983-14988.

46. Tomasetti, M.; Monaco, F.; Manzella, N.; Rohlena, J.; Rohlenova, K.; Staffolani, S.; Gaetani, S.; Ciarapica, V.; Amati, M.; Bracci, M., *et al.* Microrna-126 induces autophagy by altering cell metabolism in malignant mesothelioma. *Oncotarget* **2016**, *7*, 36338-36352.

47. Dhahbi, J.M.; Atamna, H.; Boffelli, D.; Magis, W.; Spindler, S.R.; Martin, D.I. Deep sequencing reveals novel micrornas and regulation of microrna expression during cell senescence. *PLoS One* **2011**, *6*, e20509.

48. Wu, J.; Ji, X.; Zhu, L.; Jiang, Q.; Wen, Z.; Xu, S.; Shao, W.; Cai, J.; Du, Q.; Zhu, Y., *et al.* Up-regulation of microrna-1290 impairs cytokinesis and affects the reprogramming of colon cancer cells. *Cancer Lett.* **2013**, *329*, 155-163.

49. Lewis, B.P.; Shih, I.H.; Jones-Rhoades, M.W.; Bartel, D.P.; Burge, C.B. Prediction of mammalian microrna targets. *Cell* **2003**, *115*, 787-798.

50. Krek, A.; Grun, D.; Poy, M.N.; Wolf, R.; Rosenberg, L.; Epstein, E.J.; MacMenamin, P.; da Piedade, I.; Gunsalus, K.C.; Stoffel, M., *et al.* Combinatorial microrna target predictions. *Nat. Genet.* **2005**, *37*, 495-500.

51. Bisceglie, F.; Pinelli, S.; Alinovi, R.; Goldoni, M.; Mutti, A.; Camerini, A.; Piola, L.; Tarasconi, P.; Pelosi, G. Cinnamaldehyde and cuminaldehyde thiosemicarbazones and their copper(ii) and nickel(ii) complexes: A study to understand their biological activity. *J. Inorg. Biochem.* **2014**, *140*, 111-125.
52. Livak, K.J.; Schmittgen, T.D. Analysis of relative gene expression data using real-time quantitative pcr and the 2(-delta delta c(t)) method. *Methods* **2001**, *25*, 402-408.